

# **High Temperature Viscosity Measurements by the Gas Film Levitation Technique: Application to Various Types of Materials<sup>1</sup>**

**P. H. Haumesser,<sup>2</sup> J. P. Garandet,<sup>2, 3</sup> J. Bancillon,<sup>2</sup> M. Daniel,<sup>2</sup>  
I. Campbell,<sup>4</sup> and P. Jackson<sup>4</sup>**

---

The objective of this paper is to show the potential of gas film levitation for noncontact viscosity measurements. Materials studied include oxide and metallic glasses, ceramics, and biphasic metallic alloys. After a brief presentation of the gas film levitator, the analysis procedure of the drop relaxation, both in the aperiodic and oscillating modes, is described in connection with existing hydrodynamic models. The uncertainty of the viscosity measurements ranges from 5 to 15%, depending on the type of materials. The surface tension and the mass density of the sample necessary to derive the viscosity can also be measured in the same experimental apparatus.

---

**KEY WORDS:** ceramic glazes; metallic glasses; oxide glasses; viscosity measurement.

## **1. INTRODUCTION**

A knowledge of viscosity is of high importance in a variety of processes, e.g., in the glass or ceramic industries, as well as in metallurgy. Standard techniques, such as the Couette viscometer, are generally suitable at low temperatures. However, the interaction between the crucible and the fluid may cause a number of problems, such as pollution or nucleation of spurious grains in undercooled liquids. Contactless techniques, e.g., electromagnetic [1] or electrostatic [2] levitation, have been fruitfully used at

---

<sup>1</sup> Paper presented at the Sixth International Workshop on Subsecond Thermophysics, September 26–28, 2001, Leoben, Austria.

<sup>2</sup> DRT/DTEN/SMP/LESA, CEA–Grenoble, 17 rue des Martyrs, F-38054 Grenoble Cedex, France.

<sup>3</sup> To whom correspondence should be addressed. E-mail: garandet@chartreuse.cea.fr

<sup>4</sup> CERAM, Queens Road, Stoke on Trent ST4 SLQ, United Kingdom.

high temperatures, but these techniques have a number of limitations related to the electrical properties of the material considered along with sample dimensions.

The objective of this paper is to present a description of another contactless technique, namely gas film levitation, developed in our laboratory in CEA-Grenoble [3, 4]. This technique has, in principle, no limitations in terms of processed materials, and samples of fairly large mass (up to 200 g in the case of oxide glasses) can be routinely levitated. More precisely, the purpose of this paper will be to develop the potential of the technique in the field of viscosity determination, but it should be mentioned that other thermophysical properties, such as surface tension and mass density, can also be measured.

Section 2 will be devoted to a brief presentation of the gas film levitator, including principles and technical implementation. We shall then proceed in Section 3 to some considerations on the relaxation kinetics of deformed liquid droplets, to highlight the different (namely, aperiodic versus oscillating) modes of return to equilibrium and the procedure applied to evaluate the viscosity. Finally, a number of applications of the technique to various types of materials (oxide and metallic glasses, ceramic glazes) is presented in Section 4.

## 2. GAS FILM LEVITATION

The principle of the technique is shown in Fig. 1; a flow of inert gas (argon is often used) is forced through a porous membrane placed below the sample that is levitated. The resulting gas flow acts as a supporting

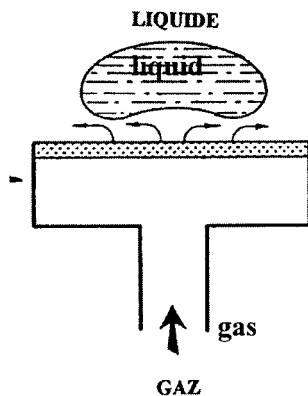


Fig. 1. Schematic diagram of levitated drop.

cushion with a typical thickness of 10 to 100  $\mu\text{m}$ . The pressure difference between the bottom and top of the porous membrane is of the order of 1 bar. For more details on the hydrodynamics of the problem, the interested reader is referred to Ref. 5, but it should be mentioned that the porous membrane is slightly concave to guarantee the lateral stability of the sample.

Regarding technical implementation, a first point to be checked concerns sample-membrane compatibility. If the material to be studied is volatile, it can evaporate and condense on the membrane, leading to a degradation of the levitation conditions. Even if the levitation takes place normally, a possible loss of mass of the material needs to be evaluated for a proper estimation of the viscosity (see Eqs. (1) and (4)). Besides, considering the limited thickness of the gas film, occasional contacts between sample and membrane are not to be excluded when the sample undergoes a change of form upon melting. Whenever possible, graphite is the preferred choice for the membrane material, due to its low cost and easy machinability, but we can also work with refractory materials (tungsten, molybdenum) or with alumina.

The viscosity measurement is based on the relaxation kinetics of a droplet contactlessly deformed from the top (see Section 3), with the help of a porous membrane similar to the one used for the levitation. The latter is connected to an hydraulic jack that allows its sudden rise (within 5 ms) at the beginning of the measurement. Both porous membranes and sample are surrounded by a thermal insulator for temperature homogenization, as can be seen in Fig. 2. Heating is achieved by means of a radio frequency system, coupling taking place either directly on the membranes or on a graphite piece holding the membranes, for the case where the latter are electrically insulating.

The temperature is controlled by means of a Type-B thermocouple located against the sustentation membrane, and the temperature is also measured at the top membrane with another Type-B thermocouple. A significant difference (of the order of 20 K) exists between these two thermocouples, which can be explained by the fact that the RF-system may heat asymmetrically the top and bottom parts of the experimental chamber. In any case, a pyrometric calibration was carried out using a graphite dummy sample in order to relate sample and regulation temperature. We also performed experiments on pure metals (Zn, Ag, Cu and Ni) of known melting point, the conclusion of the calibration procedure being that the temperatures measured in the course of the present work have an uncertainty of  $\pm 5$  K [6].

A hole in the chamber wall allows sample illumination by means of an optical fiber. The specimen is observed by means of a video camera through another hole located opposite to the illumination fiber. For

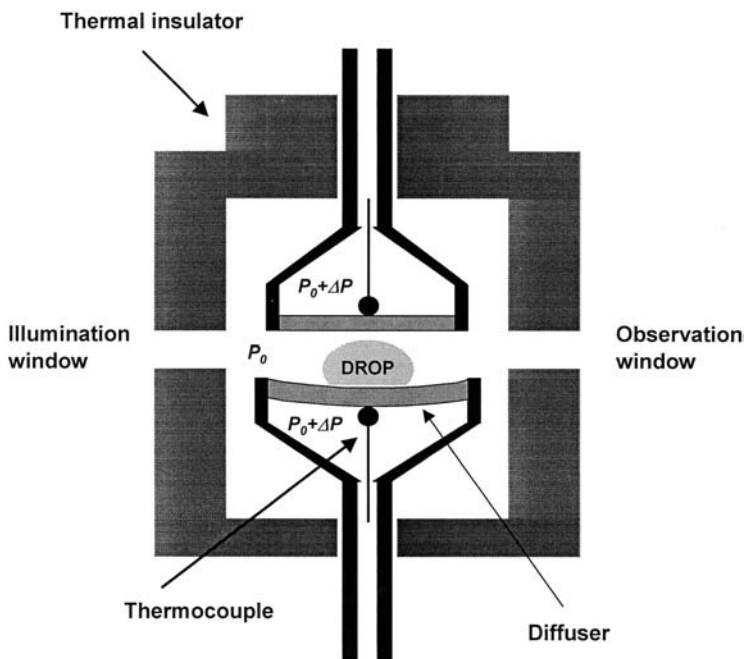


Fig. 2. Schematic showing main features of the experiment.

the case of relatively viscous materials, the relaxation kinetics are fairly slow and a standard (50 images/s) camera is sufficient, as will be seen in Sections 3 and 4. On the other hand, low viscosity materials require a fast (500 images/s) camera for a meaningful record of the relaxation. For more details on the developed apparatus, the reader is referred to Ref. 6.

### 3. PRINCIPLES OF VISCOSITY MEASUREMENT

The oscillation and damping modes of free droplets have been the subject of a number of theoretical studies since the pioneering work of Lord Rayleigh (see, e.g., Refs. 7–10). For our present purposes, the relaxation kinetics of a deformed drop can be best studied within the frame of Chandrasekhar's formalism [8], that allows the identification of two types of behavior depending on the value of the Ohnesorge number,  $Oh = \eta^2 / (R\sigma\rho)$  that relates a typical sample dimension  $R$ , and the material surface tension  $\sigma$ , density  $\rho$ , and dynamic viscosity  $\eta$ .

At high values of the Ohnesorge number, the return to equilibrium is exponential, with a characteristic time  $\tau$  proportional to the viscosity of the

material. In principle, an infinite number of harmonics should be considered to account for the relaxation kinetics, but we assumed that only the lowest excitation mode of the drop is involved. Two facts support this assumption: first, it can be shown theoretically that this mode has the slowest decay, and second the excitation procedure (sample deformation from above) is such that most energy is transferred to this mode. Combining the results of Refs. 11 and 12, the relation between  $\eta$  and  $\tau$  takes the form:

$$\eta = (20/19)(\sigma/R) C_1(f) \tau \quad (1)$$

A correction factor  $C_1(f)$  based on physical arguments has been introduced in Ref. 11 to account for the nonspherical shape of the liquid sample and for the fact that only the top of the drop participates in the relaxation. In that case, the sample equivalent radius  $R$  is defined from the sample mass  $m$  as  $R = [(3/4\pi)(m/\rho)]^{1/3}$ .

From an experimental standpoint, the important feature is that the drop apex  $h(t)$  follows an exponential curve (see Fig. 3a) from its initial value  $h_0$  (corresponding in fact to the first recorded data point) to its final (equilibrium) value  $h_\infty$ .

$$h(t) = h_\infty + (h_0 - h_\infty) \exp(-t/\tau) \quad (2)$$

The equilibrium value  $h_\infty$  is determined from the averaged drop apex position for times  $t > 6\tau$ . The nondimensional relative deformation is then defined as  $\varepsilon(t) = (h(t) - h_\infty)/(h_0 - h_\infty)$ , and the time constant  $\tau$  is evaluated from a plot of  $\ln(\varepsilon(t))$  as a function of time as can be seen in Fig. 3b.

At low values of the Ohnesorge number, the return to equilibrium of the drop apex takes the form of a damped oscillation of frequency  $\omega$  and characteristic time constant  $\tau$  scaling inversely proportional to the viscosity:

$$h(t) = h_\infty + (h_0 - h_\infty) \cos(\omega t + \varphi) \exp(-t/\tau) \quad (3)$$

$$\eta = (1/5)(\rho R^2/\tau) C_2(f) \quad (4)$$

Again, a correcting factor  $C_2(f)$  has to be introduced to account for the differences with the Chandrasekhar model. It should be mentioned that both  $C_1(f)$  and  $C_2(f)$  are not empirical quantities, but the outcome of a physical model where the drop is considered to behave as a viscoelastic element [11]. Both  $C_1(f)$  and  $C_2(f)$  are tabulated in Ref. 6.

A typical damped oscillation relaxation curve is presented in Fig. 4a. Briefly stated, the signal analysis procedure is as follows: the equilibrium value  $h_\infty$  is determined by summation of the recorded drop apex position

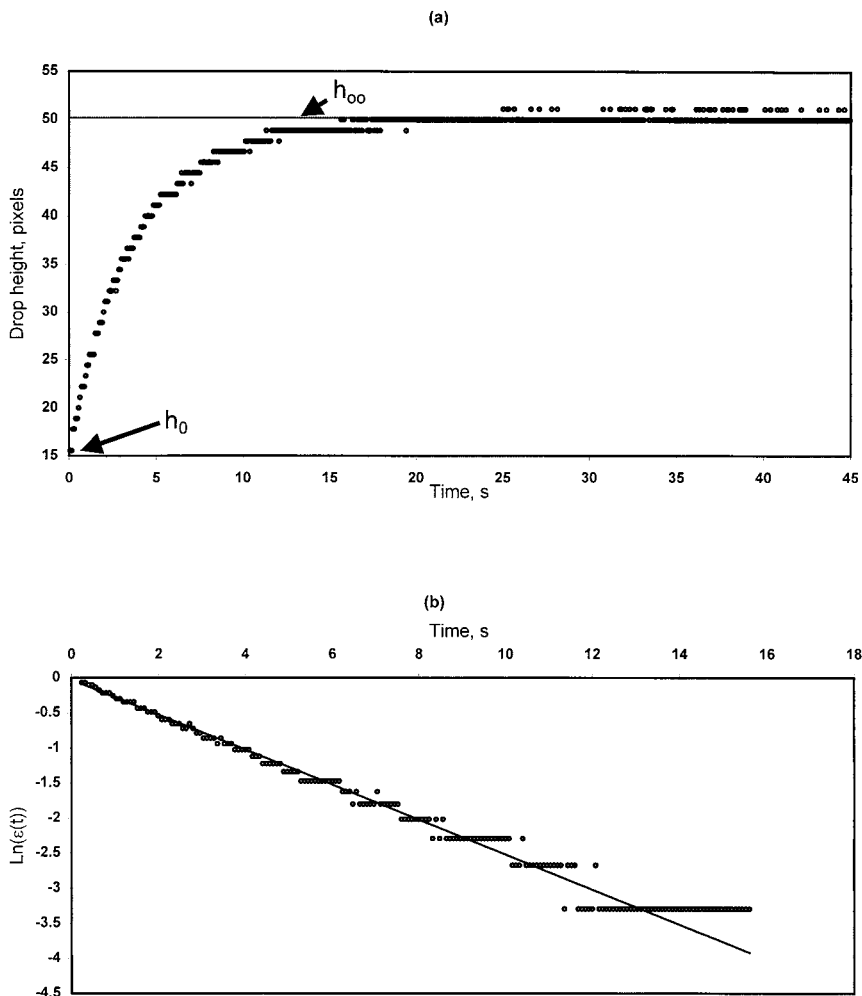


Fig. 3. Relaxation curve in (a) natural coordinates and (b) logarithm of the normalized deformation in the case of the REF710a soda-lime-silica standard glass at 1040°C.

for all experimental data points, and the identification of the local maxima is carried out on the quantity  $h'(t) = |h(t) - h_{\infty}|$  (see Fig. 4b). Keeping only these identified maxima, the nondimensional relative deformation is again defined as  $\varepsilon(t) = (h'(t) - h_{\infty}) / (h_0 - h_{\infty})$ , and the time constant  $\tau$  is evaluated from a plot of  $\ln(\varepsilon(t))$  as a function of time as for the case of the aperiodic relaxation.

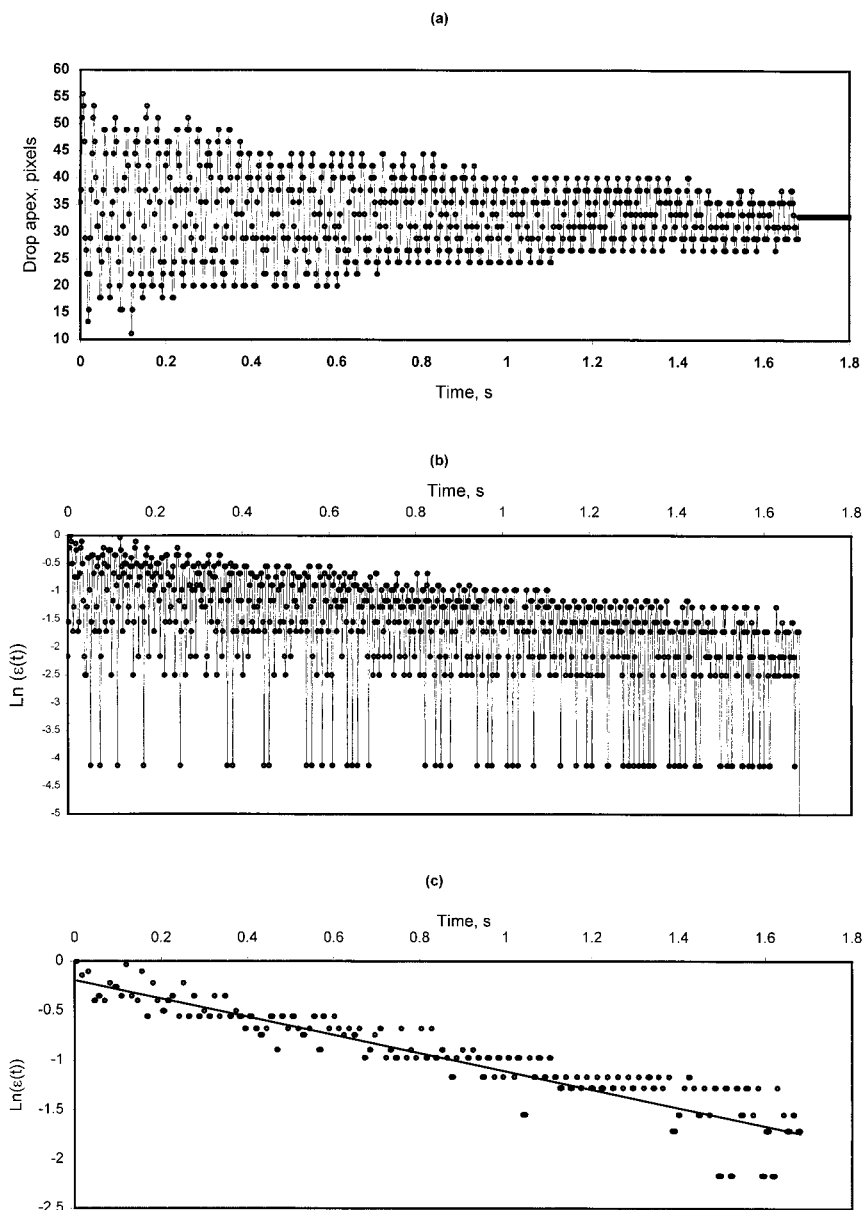


Fig. 4. Relaxation curve in (a) natural coordinates and (b) logarithm of the normalized deformation in the case of the  $\text{Pd}_{40}\text{Ni}_{10}\text{Cu}_{30}\text{P}_{20}$  glass at  $700^\circ\text{C}$ .

It should be mentioned that at low values of the Ohnesorge number, what is actually measured is the kinematic viscosity  $\nu = \eta/\rho$ . Depending on the end-user applications, either  $\nu$  or  $\eta$  may be more interesting, but an interesting feature of our experiment is that it allows an independent determination of the mass density  $\rho$  and the surface tension  $\sigma$  of the material through a best fit analysis of the equilibrium drop shape once the relaxation is completed.

As for the global accuracy of the viscosity measurement, it depends on the uncertainties of both the evaluated time constant  $\tau$  and the required thermophysical property ( $\rho$  or  $\sigma$ ). Regarding  $\tau$ , a meaningful error bar can be ascribed to the measurement using standard theorems of statistics [13] since we deal with a linear fit. In the aperiodic relaxation mode, all the recorded data points are used in the fitting procedure, and the uncertainty  $\Delta\tau/\tau$  can be as low as 2%.

In the oscillating mode on the other hand, the number of useful data points is much smaller, as only the maxima take part in the fitting procedure. Besides, lateral oscillations are sometimes observed, due to the low viscosity of the drop. These facts lead to a significantly larger uncertainty on  $\Delta\tau/\tau$ , typically of the order of 10%. Adding in the uncertainty on  $\rho$  or  $\sigma$ , typically of the order of 2%, it can be stated that the overall uncertainty of the viscosity measurements ranges from 5 to 15%, depending on the relaxation mode.

It should be noted that control of the gaseous atmosphere in our experimental setup is not fully optimized, meaning that the surface tension estimate may not be equal to the true thermodynamic value. This is specially the case for oxygen sensitive materials such as metals or semiconductors. However, most important for our present purposes, this estimate corresponds to the true physical driving force for the return to equilibrium. As such, the viscosity measurement is certainly reliable.

## 4. APPLICATIONS

### 4.1. Oxide Glasses

Experiments were carried out as part of a collaboration with Corning S.A. In all cases, the materials were sufficiently viscous for the relaxation to always occur in the aperiodic mode. The results obtained on the BL131295 sodalime glass are summarized in Fig. 5, and compare favorably (within 5%) with the results obtained by Corning using a Couette viscometer. It can be seen that our experiments cover a large temperature-viscosity range, allowing the application of fitting models, such as the well-known Vogel–



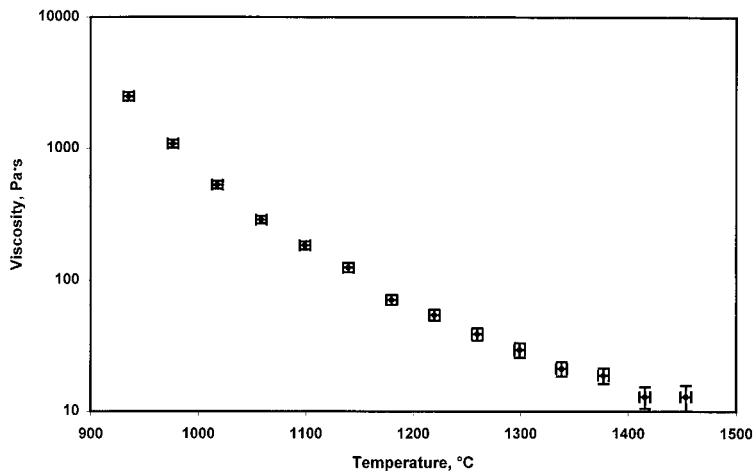


Fig. 5. Viscosity versus temperature for the BL131295 glass.

Fulcher–Tamman (VFT) model. At high temperatures, the presence of bubbles coming from the dissociation of the chemical bonds cannot be excluded. Bubbles induce a modification of the rheological behavior of the drop and render the interpretation of the experiment much more complex. An interesting feature of our measurement compared to standard Couette-type viscometers is that the presence of bubbles can, to some extent, be detected *in situ* through optical visualization. In practice, the two highest temperature points on the curve of Fig. 5 should therefore be used cautiously.

#### 4.2. Ceramic Glazes and Other Applications Involving the Fusion of Powdered Glass

The problem of bubbles is a key issue for the ceramic glaze materials that are investigated within the frame of the Craft “Visco” project supported by the European Union. This is because ceramic glazes are applied to specimen to be coated as powders that coalesce into a “homogeneous” glassy layer in firing. In practice, the expulsion of porosity arising from voids between glass particles is never complete and bubbles exist in the final glaze layer. The surface tension and viscosity properties of the glaze dictate the degree of bubble clearance during firing and hence the final appearance and in-service performance. Preliminary experiments were carried out on some forging glasses provided by Ceram in the form of pressed powders. In some cases, the size dispersion of the powder grains is

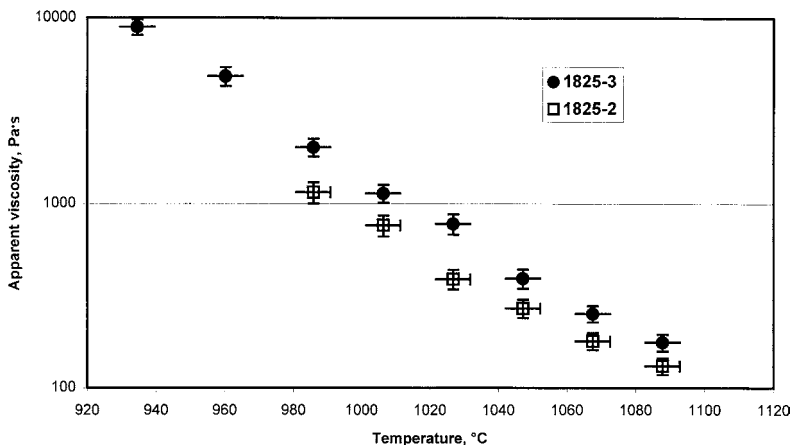


Fig. 6. Temperature variation of the apparent viscosity in two forging glasses with various bubble volume contents (1825-2:4%, 1825-3:15%).

such that they can be directly levitated in a “sand castle” configuration. However, the drop formed upon heating above the melting point contains a large volume fraction of entrapped bubbles.

Even when sintering is performed on the pressed powders to densify the sample, as performed by Ceram, the bubble volume content is of the order of 15% at the working temperature. This content can be reduced by maintaining the sample at a high temperature within the experimental device, and we managed to reach bubble volume fractions of only 4%. The results summarized in Fig. 6 show that the apparent viscosity thus obtained increases with increasing bubble content. It should be understood that such an apparent viscosity is only used as a characteristic of the rheological behavior of the deformed drops, and cannot be easily related to the true viscosity of the bubble free material. Surprisingly enough, even though the measured viscosities are quite different, the temperature variations follow a similar trend. In any case, more work is necessary to obtain bubbles-free samples to perform reference measurements.

### 4.3. Metallic Glasses

Preliminary experiments were carried out on the glass-forming system  $\text{Pd}_{40}\text{Ni}_{10}\text{Cu}_{30}\text{P}_{20}$ , the samples being provided by DLR Cologne. Such glass forming alloys have viscosities much higher than typical metals, but are still low enough for the relaxation to occur by means of damped oscillations (see Fig. 4). The viscosity versus temperature results are summarized in Fig. 7. It is indeed seen that the measured values are much higher than for

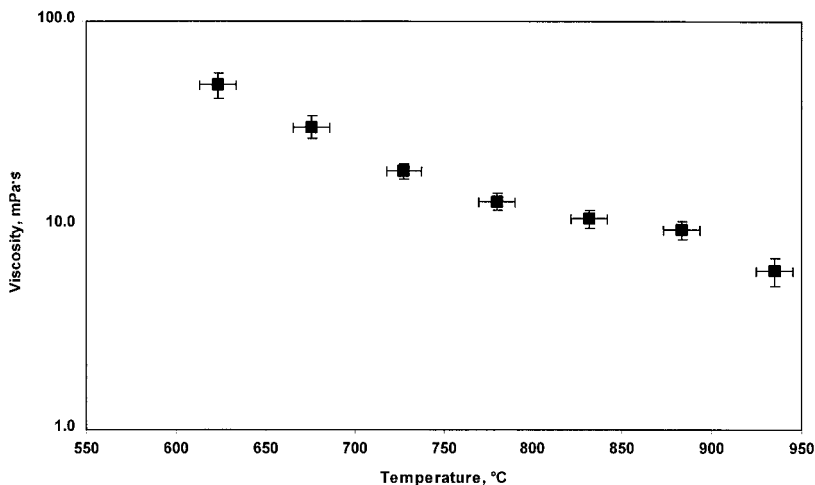


Fig. 7. Viscosity versus temperature curve of the  $\text{Pd}_{40}\text{Ni}_{10}\text{Cu}_{30}\text{P}_{20}$  metallic glass.

standard metals, and it should be mentioned that such high viscosities translate into slow atomic mobility. As such, viscosity measurements are an interesting diagnostic to characterize the glass forming ability of a given system.

## 5. CONCLUSION

The basic principles and a number of applications of noncontact viscosity measurements by the gas-film levitation technique have been presented. The results demonstrate that the technique is well adapted to the analysis of the drop relaxation method, in both the aperiodic and oscillating modes. Materials studied include oxide and metallic glasses, ceramics, and biphasic metallic alloys. The uncertainty of the viscosity measurements ranges from 5 to 15%, depending on the type of materials and the relaxation mode. An interesting feature of our experiment is that it can also be used to estimate the surface tension and the mass density of the sample in the same experimental apparatus. Provided that a porous membrane compatible with the material to be studied can be found, our technique thus appears as a suitable way to perform noncontact, high temperature viscosity measurements.

## ACKNOWLEDGMENTS

This work has been supported by the European Union (Craft Project Visco G6ST-CT-2000-50048). Thanks are due to A. Kerdoncuff and

T. Kaing from Corning SA and to I. R. Lu and G. Mathiak from DLR Cologne, respectively, for the procurement of the sodalime glasses and Bulk Metallic Glasses samples. The support from GBX company is also gratefully acknowledged.

## REFERENCES

1. I. Egry and S. Sauerland, *Mater. Sci. Eng. A* **178**:73 (1994).
2. P. F. Paradis and W. K. Rhim, *J. Mater. Res.* **14**:3713 (1999).
3. J. Granier and C. Potard, Proc. 6th Eur. Symp. Materials Sciences Microgravity Conditions, *ESA Symp. Series SP-256*:421 (1987).
4. J. C. Barbé, Ph.D. thesis (Institut National Polytechnique de Grenoble, 2000).
5. Dah Chen Sun, *J. Lubrication Tech. ASME Trans.* **95**:457 (1973).
6. P. H. Haumesser, J. Bancillon, M. Daniel, M. Perez, and J. P. Garandet, *Rev. Sci. Instrum.* (in press).
7. Lord Rayleigh, *Proc. Roy. Soc. London* **29**:71 (1879).
8. S. Chandrasekhar, *Hydrodynamic and Hydromagnetic Stability* (Pergamon Press, Oxford, 1990).
9. O. A. Basaran, *J. Fluid Mech.* **241**:169 (1992).
10. M. Papoular and C. Parayre, *Phys. Rev. Lett.* **78**:2120 (1997).
11. M. Perez, Y. Bréchet, L. Salvo, M. Papoular, and M. Suéry, *Euro. Phys. Lett.* **47**:189 (1999).
12. J. C. Barbé, C. Parayre, M. Daniel, M. Papoular, and N. Kernevez, *Int. J. Thermophys.* **20**:1071 (1999).
13. See, e.g., *Numerical Recipes in C: The Art of Scientific Computing* (Cambridge University Press, 1992), Chap. 15.